

Experimental Investigation of End Plate Effects on the Vertical Axis Wind Turbine Airfoil Blade

Rikhi Ramkissoon¹, Krishpersad Manohar²Ph.D. Candidate, Department of Mechanical and Manufacturing Engineering, The University of the West Indies,
St. Augustine, Trinidad, West Indies¹Senior Lecturer, Department of Mechanical and Manufacturing Engineering, The University of the West Indies,
St. Augustine, Trinidad, West Indies²

ABSTRACT: An experimental investigation of the variation of lift coefficient at low wind speeds comparative to the operation of a vertical axis wind turbine operation was undertaken. Data was recorded at angle of attack for $\pm 0, 5, -5, 10, -10, 15, -15$ degrees and the wind speed was varied for Reynolds number ranging from 3.32×10^5 to 9.64×10^5 . Pressure taps on the airfoil skin collected the stagnation pressures which were converted to lift coefficient values. Experiments were conducted with and without end plate attachment to the MI-VAWT1 airfoil. Results indicated that the addition of the endplates increased the lift coefficient at all angle of attack over the range of Reynolds number tested. Similar trends were observed with and without endplate. The flow regime boundary layer separation point advanced toward the leading-edge with an increase in the angle of attack up to $\pm 10^\circ$. As the angle of attack increased above $\pm 10^\circ$ the stall angle was approached. This resulted in the separation bubble bursting, which created a suction peak and the lift coefficient decreased.

KEYWORDS: Lift coefficient, Endplates, Vertical axis wind turbine, Airfoil.

I. INTRODUCTION

For centuries wind turbines served as a practical way to capture and convert the kinetic energy of the wind to mechanical and in more recent times directly to electrical energy. The straight bladed Darrieus vertical axis wind turbine (VAWT) is very attractive for its low cost and simple design [1]. Selection of airfoil was one of the most critical factors in achieving better aerodynamic performance and in determining the optimum dimensions of a fixed-pitch straight-bladed Darrieus type vertical axis wind turbine (SB-VAWT), along with solidity, radial arm parasitic drag, aspect ratio [2]. Also, airfoil related design changes has the potential for increasing the cost effectiveness of SB-VAWTs making them prospective candidates for diversified urban and rural applications. It has been shown that conventionally-used old NACA 4-digit symmetric airfoils were not suitable for smaller capacity SB-VAWT [3]. Rather, it was advantageous to utilize a high-lift and low-drag asymmetric thick airfoil suitable for low speed operation typically encountered by SB-VAWT. A special purpose airfoil called the MI-VAWT1 was designed by M. Islam, D. Ting and A. Fartaj from the University of Windsor, Windsor, Ontario, Canada in 2007 to satisfy the low speed VAWT operating conditions [3, 4]. In this study the performance enhancement characteristic with the addition of end plates to the MI-VAWT1 airfoil was investigated.

II. MI-VAWT 1 AIRFOIL

To investigate the improved the performance of the straight-bladed vertical axis wind turbine (SB-VAWT) by the addition of end plates, a sensitivity analyses was conducted with different geometric features to understand the effects

International Journal of Innovative Research in Science, Engineering and Technology

(A High Impact Factor, Monthly Peer Reviewed Journal)

Vol. 5, Issue 2, February 2016

on performance. Subsequently, the special purpose airfoil “MI-VAWT1” was replicated utilizing the XFOIL software with the computational scheme developed by Islam et al [3, 4]. Figure 1 shows a schematic of the MI-VAWT1 airfoil.

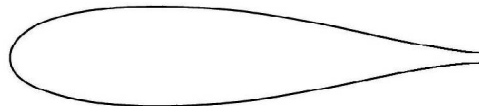


Fig. 1. MI-VAWT airfoil (Islam, Ting, and Fartaj 2007) [3, 4].

The performance of the MI-VAWT1 was superior when compared with that of NACA 0015 and LS-0417 at different Reynolds numbers [3]. Also, the C_{pnet} values were higher and the $C_{Qnet}-\lambda$ curves showed superior performance.

III. ENDPLATE

It is well established that tip vortex caused downwash that modified the pressure distribution on the airfoil surface and increased the induced drag [5]. Tip vortices modify the local flow-field by creating an induced horizontal velocity that decreased the local angle of attack. The total drag coefficient, C_D , for a wing can be expressed by:

$$C_D = C_{D,p} + C_{D,f} + \frac{C_L^2}{(\pi \cdot e \cdot AR)} \quad (1)$$

where e is the span efficiency, $C_{D,p}$ is the drag component of the total aerodynamic force over the wing surface, $C_{D,f}$ is the drag caused by friction, AR is the aspect ratio, and $\frac{C_L^2}{(\pi \cdot e \cdot AR)}$ is the induced drag [6].

The use of endplate deterred the flow from the high pressure region on the airfoil to reach the low pressure region on the outside of the wing. Also, the endplate slowed down the flow near the airfoil tip. This decrease in velocity reduced the pressure drop on the low pressure side of the wing corresponding to the vortex core.

IV. MI-VAWT1 AIRFOIL MODEL DESIGN

A MI-VAWT1 aluminum airfoil model was fabricated with the following characteristics:

- Chord length, $c = 0.20$ m
- Span, $b = 0.16$ m
- Aspect ratio, $AR = 0.8:1$
- Chord-to-tunnel height, $c/h = 0.33$
- Endplate of MI-VAWT1 profile (Chord length 0.25 m).

The model was tested in an open-circuit suction wind tunnel in which the airflow was completely contained within the wind tunnel laboratory [7]. The air leaving the wind tunnel via the fan flowed through the laboratory room and back through a filter and screen into the wind tunnel. The wind tunnel was the conventional non-return type with one closed working section and was constructed using 9.49 mm thick plywood. The dimension of the wind tunnel was 3.9116 m in overall length, 1.6256 m wide and 1.6256 m high at the mouth [7, 8].

The model was mounted horizontally in the test section 2 m downstream of the contraction, spanning the entire width of the test section. The airfoil skin made out of 16-gauge aluminum sheet metal was drilled to facilitate the required installation of static pressure taps. Six (6) tapped holes were drilled on the surfaces of the 16-gauge aluminum sheet metal to attach the skin to the airfoil support. Countersunk screws were used to secure the sheet metal to the interface plates (Figure 2).

International Journal of Innovative Research in Science, Engineering and Technology

(A High Impact Factor, Monthly Peer Reviewed Journal)

Vol. 5, Issue 2, February 2016

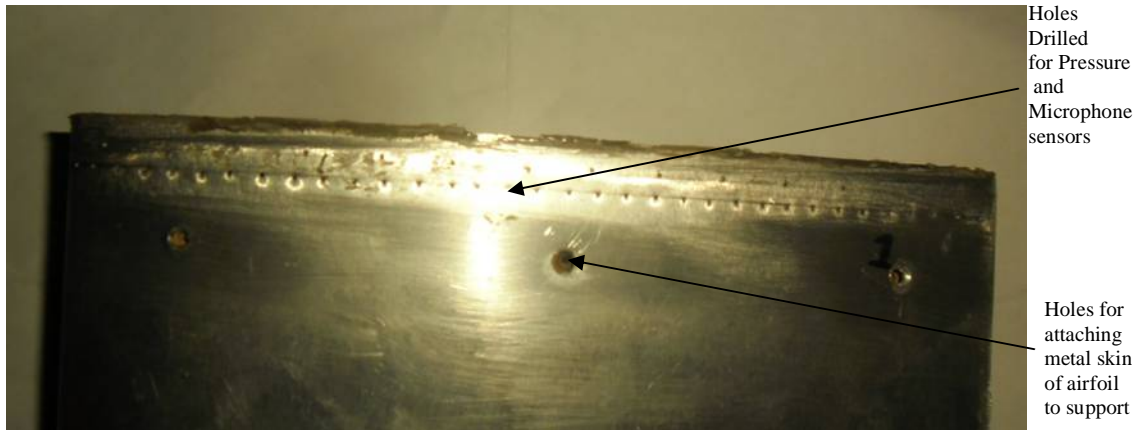


Fig. 2. Pressure sensor, microphone and attaching holes drilled on the surface of the 16-gauge aluminum sheet metal skin of the airfoil.

A relatively high concentration of pressure taps near the leading-edge was necessary to measure the steep pressure gradients in this region. Conversely, a lower concentration of pressure taps was acceptable near the trailing-edge since the pressure recovery was gradual in that region [9]. A total of 58 pressure taps symmetrically distributed on the upper and lower surfaces along the mid-span of the model provide an optimum degree of resolution within practical constraints (Figure 2). To facilitate measurements of time-resolved fluctuating surface pressure, pressure transducers are embedded in the airfoil surface. Twenty two (22) pressure transducers were allocated in 1 row, spanning the extent of the MI-VAWT1 airfoil skin. All countersunk screw holes drilled into the skin were smoothed down.

An automated data acquisition system was used to acquire static surface pressure measurements sequentially from all the static pressure taps on the airfoil skin. LabVIEW software was used to acquire and log all pressure measurements within the test section. Pressure measurements were performed with a calibrated electronic pressure scanner module (Scanivalve ZOC22b). All digital signals sent to the pressure scanner modules and auxiliary systems (i.e., to specify the binary logic state) were controlled from a PC with a National Instruments PCI 6259 data acquisition card (DAQ). An NI SCB-68 connector block (Figure 3) was used to connect the ZOC22b pressure scanning module to the PCI 6259 DAQ card.

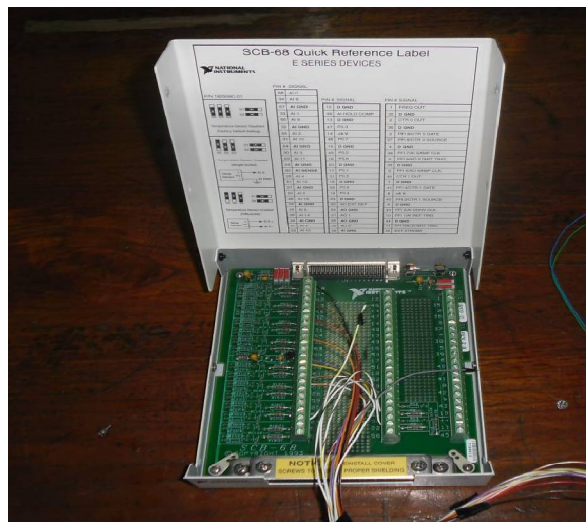


Fig. 3. NI SCB 68 connector block.

International Journal of Innovative Research in Science, Engineering and Technology

(A High Impact Factor, Monthly Peer Reviewed Journal)

Vol. 5, Issue 2, February 2016

V. TESTING PROCEDURE

The MI-VAWT1 airfoil with and without endplate was placed in the wind tunnel and the wind speed and angle of attack was varied. At angle of attack of 0, 5, -5, 10, -10, 15, -15 degrees the wind speed was varied for Reynolds number ranging from 3.32×10^5 to 9.64×10^5 , and the corresponding data recorded. Pressure taps on the airfoil skin collected the stagnation pressures which were then converted to lift coefficient values (Figure 4).



Fig. 4. Pressure lines and microphones attached to airfoil skin.

A total of 28 sets of experiments were carried out, one at each of the four Reynolds number and the seven angle of attack for the MI-VAWT1 airfoil without endplate (Figure 5) and another 28 sets of experiments were carried out MI-VAWT1 airfoil with endplate. All measurements made were at steady state conditions and atmospheric pressure and temperature variation was within 2.0%. The chord of the endplate was 25 cm. The model was mounted horizontally in the test section 2 m downstream of the contraction, spanning the entire width of the test section [10].

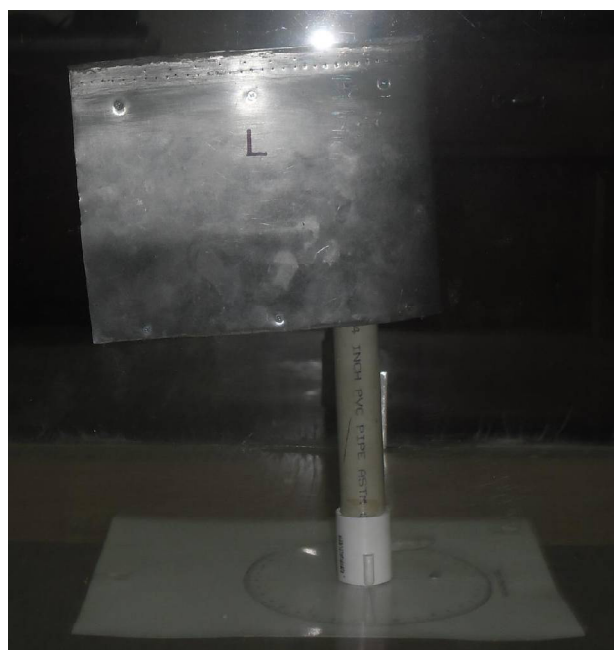


Fig. 5. The MI-VAWT fully instrumented airfoil model without end plates.

International Journal of Innovative Research in Science, Engineering and Technology

(A High Impact Factor, Monthly Peer Reviewed Journal)

Vol. 5, Issue 2, February 2016

VI. RESULTS

The average of the 28 static pressure readings data for the respective Reynolds number and angle of attack were used to calculate the corresponding pressure coefficient. These pressure coefficients were then used to calculate the lift coefficients. The lift coefficient was computed by integrating the mean surface pressure coefficient distribution using Equation 2 [11].

$$C_l = \int_0^1 (\langle C_p \rangle_{lower} - \langle C_p \rangle_{upper}) d\left(\frac{x}{c}\right) \cos \alpha \quad (2)$$

where $\langle C_p \rangle_{lower}$ and $\langle C_p \rangle_{upper}$ are the mean surface pressure coefficients on the lower and upper surfaces, respectively.

Steady state conditions existed for the testing periods and the variation in each set of reading were within 3%. After each set of experiments, the test equipment was inspected and calibration checked to ensure proper that functioning. The experimental results are shown on tables 1 and 2.

Table 1. Comparative data for Experimental Lift Coefficient with and without endplate attached for 0 to 15 degrees.

Re	AoA	C_l With Endplate	C_l Without Endplate	% Increase
3.32 x 10 ⁵	0	0	0	
	5	0.681	0.661	2.94
	10	1.39	1.31	5.76
	15	0.41	0.38	7.32
5.32 x 10 ⁵	0	0	0	
	5	0.66	0.64	3.03
	10	1.37	1.32	3.65
	15	0.38	0.34	10.53
7.31 x 10 ⁵	0	0	0	
	5	0.63	0.62	1.59
	10	1.4	1.35	3.57
	15	0.4	0.36	10.00
9.64 x 10 ⁵	0	0	0	
	5	0.62	0.61	1.61
	10	1.41	1.37	2.84
	15	0.43	0.37	13.95

International Journal of Innovative Research in Science, Engineering and Technology

(A High Impact Factor, Monthly Peer Reviewed Journal)

Vol. 5, Issue 2, February 2016

Table 2. Comparative data for Experimental Lift Coefficient with and without endplate attached at 0 to -15 degrees.

Re	AoA	C_l With Endplate	C_l Without Endplate	% Increase
3.32×10^5	0	0	0	
	-5	-0.618	-0.632	2.22
	-10	-1.157	-1.214	4.69
	-15	-0.884	-0.941	6.06
5.32×10^5	0	0	0	
	-5	-0.662	-0.675	1.93
	-10	-1.233	-1.287	4.20
	-15	-0.908	-0.962	5.61
7.31×10^5	0	0	0	
	-5	-0.678	-0.694	2.31
	-10	-1.243	-1.294	3.94
	-15	-0.919	-0.971	5.36
9.64×10^5	0	0	0	
	-5	-0.692	-0.704	1.70
	-10	-1.251	-1.296	3.47
	-15	-0.939	-0.982	4.38

VII. DISCUSSION AND CONCLUSION

In general the addition of the endplates increased the lift coefficient at all angle of attack over the range of Reynolds number tested as shown on table 1 and 2.

When the experiments were conducted with the endplate attached to the MI VAWT-1 airfoil similar trends were observed as without the endplate attached. The test results indicated that the flow regime of boundary layer separation point advanced toward the leading-edge with an increase in the angle of attack up to $\pm 10^\circ$ [12]. This resulted in the increased lift coefficient values for both with and without end plates. As the angle of attack increased above $\pm 10^\circ$ the stall angle was approached. This resulted in the separation bubble bursting, which created a suction peak and the lift coefficient decreased [13].

REFERENCES

- [1] Manohar, K., "Hybrid Lift-Drag Wind Turbine", International Journal of Applied Engineering Research, vol. 5, no. 14, pp. 2425-2434, 2010.
- [2] Ramkissoon, R. and Manohar K., "Increasing the Power Output of the Darrieus Vertical Axis Wind Turbine." British Journal of Applied Science & Technology, vol. 3, no. 1, pp. 77-90, 2013.
- [3] Islam, M., Ting, D., and Fartaj, A., "Desirable Airfoil Features for Smaller-Capacity Straight-Bladed VAWT." Wind Engineering vol. 31, no. 3, pp. 165-196, 2007

International Journal of Innovative Research in Science, Engineering and Technology

(A High Impact Factor, Monthly Peer Reviewed Journal)

Vol. 5, Issue 2, February 2016

- [4] Islam, M., Ting, D., and Fartaj, A., "Design of a special purpose Airfoil for Smaller-Capacity Straight-Bladed VAWT." *Wind Engineering* vol. 31, no. 6, pp. 401-424, 2007.
- [5] Norberg, C., "Interaction Between Freestream Turbulence and Vortex Shedding for a Single Tube in Cross-Flow." *Journal of Wind Engineering and Industrial Aerodynamics*, vol. 23, pp. 501-514, 1986.
- [6] Donald, R. R., "Wind Tunnel Investigation and Analysis of the Effects of Endplates on the Aerodynamic Characteristics of an Unswept Wing", Langley Memorial Aeronautical Laboratory. Technical note 2440, 1951.
- [7] Ramkissoon, R., and Manohar, K., "Design and Calibration of a Low Speed Wind Tunnel", *British Journal of Applied Science and Technology*, vol.4, no. 20, pp. 2878-2890, 2014.
- [8] Manohar, K., and Ramkissoon, R., "Low Cost Laboratory Built Wind Tunnel", *International Journal of Engineering Trends and Technology*, vol. 30, no. 4, pp. 176-179, 2015.
- [9] Brooks, T., and Hodgson, T., "Trailing edge noise prediction from measured surface pressures", *Journal of Sound and Vibration*, vol. 78, no. 1, pp. 69-117, 1981.
- [10] Farabee, T. M., and Casarella, M. J., "Measurements of fluctuating wall pressure for separated/reattached boundary layer flows", *Journal of vibration, acoustics, stress, and reliability in design*, vol. 108, no.3, pp. 301-307, 1986.
- [11] Gerakopoulos, J. R., "Investigating Flow over an Airfoil at Low Reynolds Numbers Using Novel Time-Resolved Surface Pressure Measurements." Master's thesis, University of Waterloo, Ontario, Canada.2011.
- [12] Lee, I., and Sung, H. J., "Characteristics of Wall Pressure Fluctuations in Separated and Reattaching Flows Over a Backward-Facing Step." *Experiments in Fluids*, vol. 30, no. 3, pp. 262-272, 2001.
- [13] Burgmann, S., and Schröder, W., "Investigation of the vortex induced unsteadiness of a separation bubble via time-resolved and scanning PIV measurements." *Experiments in Fluids*, vol. 45, no. 4, pp. 675-691, 2008.